

## High Index Contrast Photonics Platform

Sai T. Chu, Brent E. Little, John V. Hryniewicz, Fred G. Johnson, Oliver King, Dave Gill, Wenlu Chen and Wei Chen

Little Optics Division, Nomadics Inc.  
9020 Junction Drive, Annapolis Junction, MD 20701

### Abstract

A new low-loss high-index-contrast photonics platform has been developed for integrated optics and microwave photonics. The platform consists of a material system that has an index contrast that is adjustable from 0 to 25% and which is processed using conventional CMOS tools. The platform allows one to four orders of magnitude reduction in the size of optical components compared with conventional planar technologies. As an example, meter long path lengths occupy coils that are millimeters in diameter. Microwave photonic building blocks that are enabled include large bit count programmable delay lines for beam steering and shaping that fit in less than a square centimeter and which have delays controllable from 5 fsec to 10 nsec. Also enabled are arrays of high order tunable filters, a hundred micrometers in size, having linewidths ranging from tens of MHz to tens of GHz. These filters can be tuned over several hundred GHz, and when placed in Vernier architectures can be tuned across the C band (5 THz). An optical chip typically consists of dozens of optical elements. Each element is placed in its own micro-control loop that consists of a thin film heater for thermo-optic control and a thermistor for electronic feedback. The micro-control loops impart intelligence to the optical chip.

### Introduction

In electronics, electromechanics and other fields, the desire to reduce cost, improve power consumption, simplify packaging, and to increase functionality and yield, has always been the impetus for miniaturization and integration. The reasons to miniaturize and integrate are no less compelling for optical components. Indeed, healthy sustained growth for the industry may eventually demand it. However, the intrinsic analogue nature of optical components, the lack of universal photonic building blocks, and the very demanding requirements of telecom applications have made progress towards very large scale integrated (VLSI) photonics slow. Momentum is picking up though, as versatile new materials, highly functional building blocks, and volume manufacturing know-how are being demonstrated. In [1] we speculated on the viability of VLSI Photonics. Here we highlight its realization.

The commercial realization of VLSI Photonics hinges on the conjunction of three platforms. The first is a material system that has a high refractive index contrast, is low

loss throughout the communications bands, and is processed using conventional IC industry tools. The second platform comprises ultra-compact universal building blocks that can be architected into various optical signal processing functions. The third platform is the ability to leverage volume manufacturing tools and techniques from the IC industry.

### Materials Considerations for VLSI Photonics

Large-scale integration requires the miniaturization of today's PLC components. The minimum size of a photonic circuit is limited by the bending induced losses associated with the smallest radius of curvature. Bending losses decrease exponentially with increasing core-cladding refractive index contrast ( $\Delta n$  here), making high- $\Delta n$  a fundamental requirement for VLSI Photonics. On the other hand, arbitrarily large  $\Delta n$  are not necessarily desirable. As  $\Delta n$  increases, fabrication tolerances decrease, single mode waveguide dimensions decrease making fiber coupling more difficult, and structural features such as coupling gaps become prohibitively small. Figure 1 shows the minimum bending radius as a function of index contrast (solid curve, left axis). The dashed curve and right axis in Figure 1 shows the typical propagation loss as a function of index contrast. Although this curve is not fundamental, it is a function of the state of the art in deposition and fabrication processes. A large  $\Delta n$  is only one of several requirements of a viable VLSIP materials platform. Other key material attributes include: (i) low intrinsic losses, (ii) a  $\Delta n$  that is adjustable, (iii) long term stability, (iv) compatibility with IC industry processing tools and (v) low temperature processes which avoid annealing steps.

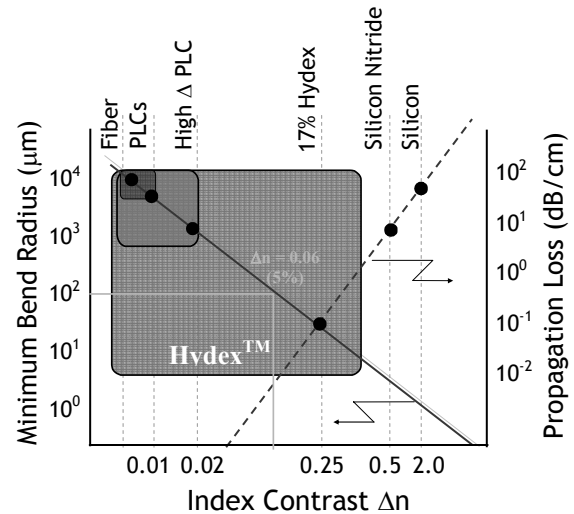


Figure 1. Minimum bend radius (left axis), and propagation loss (right axes) as a function of core-to-clad index contrast  $\Delta n$ .

Several high- $\Delta n$  material systems are being investigated for use as high index contrast photonics platforms. These include Si/SiO<sub>2</sub>, InGaAsP, Ta<sub>2</sub>O<sub>5</sub>:SiO<sub>2</sub>, SiN, SiC, SiON, and several polymeric systems. Of these Si, SiN, SiON and SiC are attractive for their long-term reliability and IC industry processing compatibility. Si and SiN have very high refractive indexes leading to extremely tight manufacturing tolerances, especially for wavelength selective applications. SiON has attracted interest because of its adjustable refractive index. In particular, its index can be made larger than that of conventional Ge-doped silica. However, SiON exhibits a strong absorption peak that extends deep into the C-band, as seen in Figure 2, and whose magnitude is a function of refractive index. Annealing is a common approach used to partially reduce the

absorption seen in material systems, (as well as to reflow cladding layers). The fate of high temperature anneals are well known: large material birefringences caused by frozen-in stresses, wafer bowing due to mismatched CTEs, and changes in refractive index and thickness affecting device performance.

Hydex™, a photonics material breakthrough, was developed to overcome the loss, reliability, and manufacturability limitations of other high- $\Delta n$  systems [2]. It is a robust material that is deposited through conventional chemical vapor deposition (CVD) processes. Its refractive index contrast is adjustable from 0% to over 20%. It requires no anneal steps and its loss as deposited, is low throughout the S, C and L bands. Three thousand hours of 85/85 damp heat testing have revealed no index changes down to the measurement accuracy of  $10^{-5}$ . In all the fabricated components described in this paper, Hydex material with a core-clad refractive index contrast of  $\Delta n=0.25$  (17% index contrast) was used. Figure 1 shows that with today's state of the art in fabrication, 17% index contrast is an optimum balance between achieving high index contrast and low propagation loss.

### Optical Components Miniaturization

An immediate application for Hydex is the ability to reduce the dimensions of all conventional PLCs by one to two orders of magnitude. This translates into a factor of ten to over a hundred more devices fabricated per wafer. An example of such miniaturization is the 40-channel, 100 GHz micro-AWG shown in Figure 3. The size of this device is approximately 5mm by 5mm and is limited solely by the pitch requirement of the 40 output fibers.

Propagation Loss Comparison  
Hydex™ vs SiON

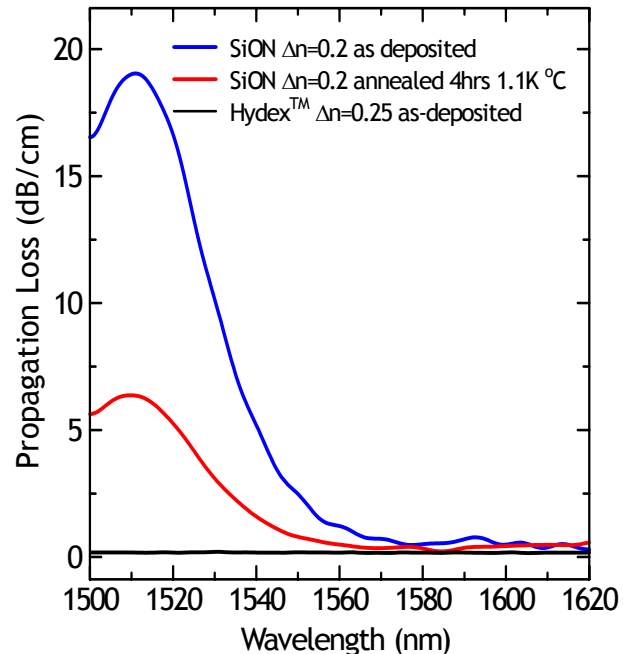


FIGURE 2. Propagation loss for silicon oxynitride and for as-deposited Hydex. Hydex™ has a loss < 0.15 dB/cm for all index values.

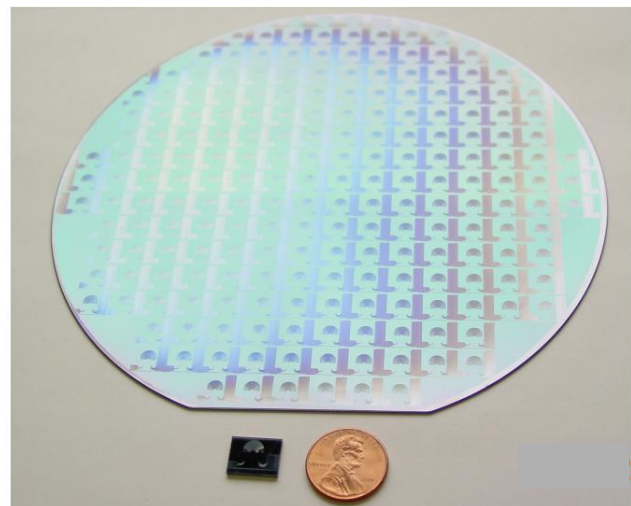


FIGURE 3. A 6" silicon wafer with over 200 40-channel 100 GHz AWGs, each with integrated spot size transformers.

The performance of these micro-PLC components is in no way compromised compared to conventional PLCs. The AWG filter noise floor for instance, which is indicative of statistical index and thickness variations in the process, is below  $-55$  dB. Indeed, the measured random phase errors in the AWG are below 8 nm, and these are repeatable from die to die across the wafer (i.e., they reside in the mask, not the process). These chips, which have compact integrated fiber spot size transformers as part of the process, exhibit fiber-to-fiber peak losses below 3 dB (for Gaussian filter shapes). An additional benefit of size reduction is the reduced power consumption for temperature stabilizing the array.

### Building Blocks in High Performance PLC Devices

An important benefit from the size reduction of conventional PLC is the possibilities of using them as components to build more sophisticated and higher performance PLC. A complete class of conventional optical elements and components has been developed using the Hydex<sup>TM</sup> platform. This includes broadband switches, Mach-Zehnder interferometer, mode size transformer and star coupler. Beside the above mentioned conventional components the high index contrast platform also enables the development of a special class of components such as microring resonators, long waveguide spirals, polarization beam splitters and polarization rotators that has much better performance and desirable characteristics than their low index contrast counterparts.

### Microring Resonator

Resonators have been used extensively in electronics for their frequency selective properties. In particular, dielectric ring and disk shaped cavities continue to be important for high frequency, high-Q microwave applications [3]. For optical signal processing applications, dielectric microring resonators have been demonstrated as demultiplexers, add/drop filters, dispersion compensators, modulators, lasers, and for four-wave mixing, to name just a few. Such devices have also been made as small as a few micrometers in size, and are thus ideal for large-scale integration.

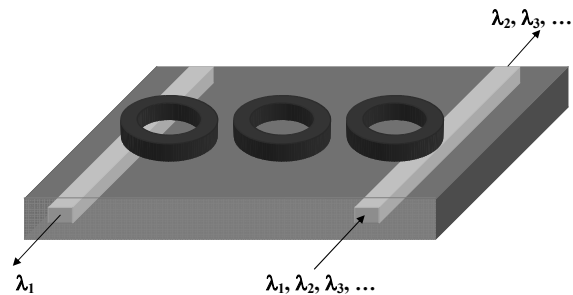


Figure 4. A coupled microring resonator building block incorporating three mutually coupled rings. The input and output bus waveguides are vertically coupled to the rings while the rings are laterally coupled to their neighbors.

A schematic of a coupled microring resonator building block is shown in Figure 4. In our preferred configuration, the rings are vertically coupled to bus waveguides, and laterally coupled to themselves. This has manufacturing advantages. Almost arbitrarily high orders can be produced with planar microring resonators, as all cavities reside in

a *single* dielectric layer, as opposed to requiring hundreds of layers as would be the case in Thin Film Filters (TFFs). Rings support traveling wave modes. This allows them to have four spatially separated ports which give them unique advantages in optical circuit architectures.

Vertical coupling is required between the outer rings and the bus waveguides in order to achieve strong coupling without requiring the realization of very narrow lateral gaps. Narrow lateral gaps are difficult to be fabricated reproducibly and can not lead to a stable manufacture process with high yields. In most applications calling for high-order (coupled cavity) filters, it turns out that the coupling strength required between rings is much smaller than the coupling strength between the rings and the straight bus guides. The net result is that the gap between two laterally coupled rings can be made large enough to be manufactured by conventional lithographic sources.

In wavelength filter applications, filter shape is paramount. Like their thin film filter counterparts, ring resonators can be arranged in coupled-cavity configurations called higher order filters. Such configurations lead to box-like response with very high out of band signal rejection. Figure 5 shows examples of fabricated filters having 1, 3, and 5 coupled cavities. Figure 6a shows experimental results for filters from order 1 to 6. In this plot the curves have all been normalized to their respective 3 dB bandwidths so that the effect on filter order can be more clearly seen. In general, the actual bandwidths range from a few GHz to several tens of GHzs. As the filter order increases, the passband shape becomes more flat, and the transition between inband and out of band increases more abruptly. The on-chip loss of higher order filters is less than 1 dB for orders up to 5<sup>th</sup> order. Figure 6b, shows the response of a fabricated 11<sup>th</sup> order filter having a very box-like response.

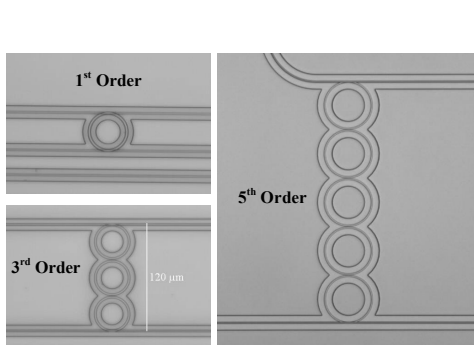


Figure 5. Examples of fabricated 1<sup>st</sup>, 3<sup>rd</sup>, and 5<sup>th</sup> order microring resonator filters. The ring radii are 20  $\mu\text{m}$  for the 1<sup>st</sup> and 3<sup>rd</sup> order filters, and 42  $\mu\text{m}$  for the 5<sup>th</sup> order filter. The core-clad refractive index contrast is 17%,

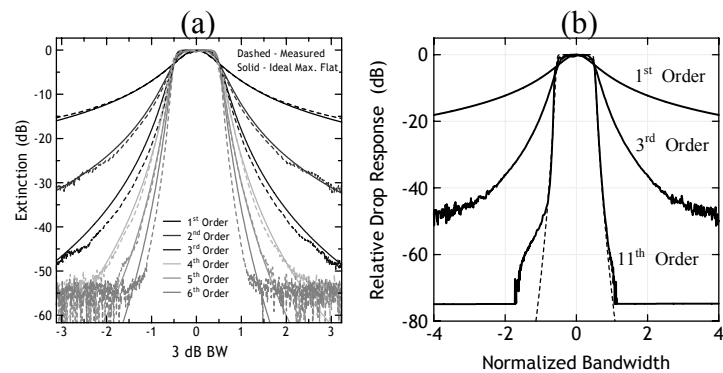


Figure 6. Examples measured responses for various filter orders. The responses have been normalized to their 3 dB bandwidths. The dashed curve in (b) is the theoretical fit.

## Tunable Filters

Rings have a temperature dependent resonance, and this can be used to increase their functionality. A thin film heater is placed over the rings, and the tuning rate is approximately  $17 \text{ pm}^\circ\text{C}$ . Because the rings lie in a two-dimensional planar geometry, the heater is equidistant from all the rings and the filter shape tunes without distortion.

Tuning a single microring based filter across the entire C-band would require prohibitively large temperature excursions. In order to overcome the need for very high temperatures, as well as overcoming an FSR that is smaller than the C-band, a Vernier architecture is used. The Vernier architecture uses a cascade filter arrangement of two or more filter stages in which the filter stages all have slightly different

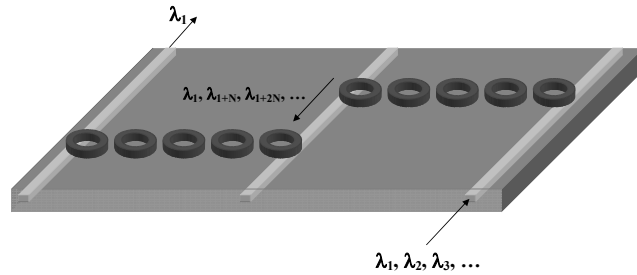


Figure 7. Schematic of a Vernier architecture composed of two sets of 5<sup>th</sup> order microring resonator filters. One filter has an FSR of 575 GHz, while the second filter has an FSR of 650 GHz.

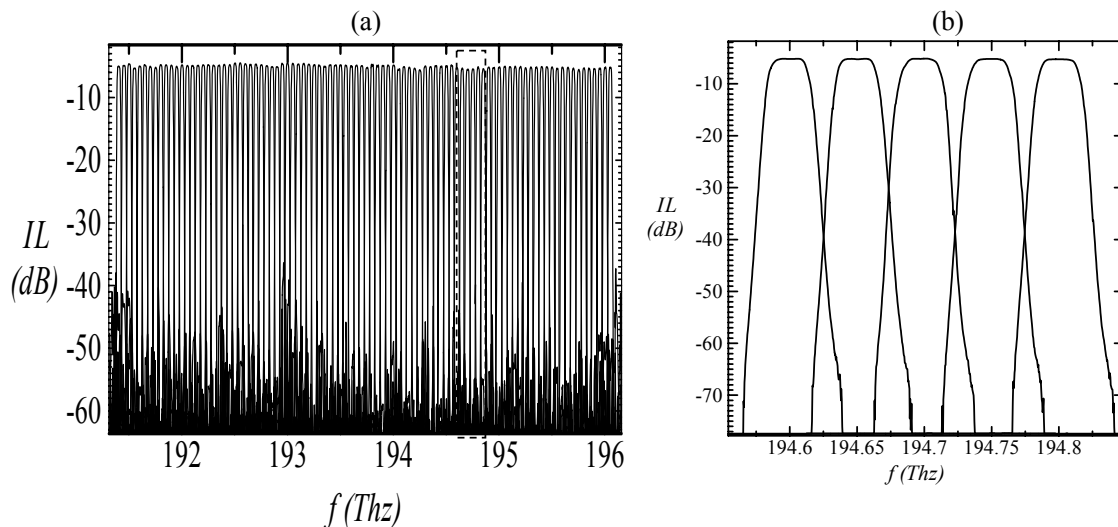


Figure 8. (a) Response of the Vernier Filter when tuned across the C-band in increments of 50 GHz. (b) Close up of the filter lineshape for several channels.

FSRs. The non-identical FSRs ensure that non-overlapping resonant peaks from each set of filters are suppressed; yielding a net FSR that is much larger than that of the individual filters. A Vernier architecture is shown in Figure 7. Figure 8a shows the filter tuned across the C-band in 50 GHz steps (100 channels), while Figure 8b shows a more detailed response of the filter shape tuned to a few consecutive channels. The fiber-to-fiber insertion loss of this device is below 4 dB. In this example, 5<sup>th</sup> order filter cells were used [4].

## Optical Code Division Multiple Access Coder/Decoder

Optical Code Division Multiple Access or OCDMA, offers the potential of increased network functionality and enhanced system security [5]. In OCDMA, data packets are spread across several spectral lines or channels, and each frequency channel has a relative phase added to it. The relative phase of all channels as a vector, represents the optical code. In a technique developed by Telcordia, the spectral phase encoding approach consists of demultiplexing the individual mode locked laser lines that make up a data signal, shifting the phase of each line according to a code, and recombining the shifted lines to produce the coded signal. Basing the OCDMA code on phase control of individual spectral lines limits the spectral bandwidth, allowing high spectral efficiency and compatibility with existing transparent WDM systems. To do so, however, requires the ability to access each of the closely spaced (10 GHz) spectral lines, to guarantee optical paths within a particular OCDMA encoder or decoder remain stable to a fraction of a wavelength, and to create the desired phase changes accurately and stably.

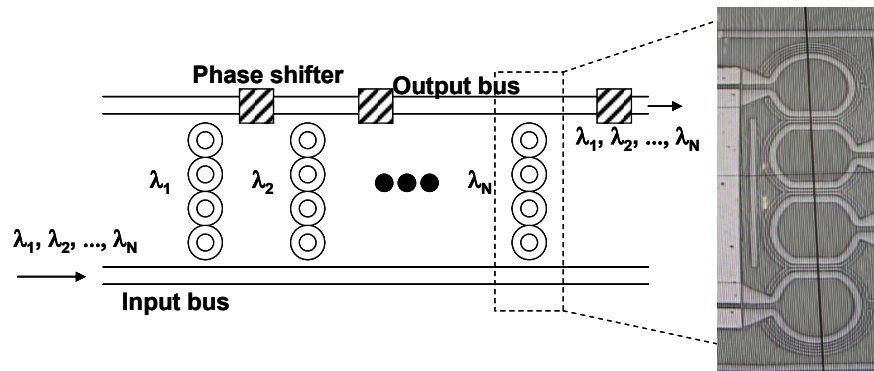


Figure 9. Schematic of the OCDMA chip, incorporating 4<sup>th</sup> order microring resonator filters. Micrograph shows the ring resonator heaters.

Microring resonator devices are ideally suited to this application, providing ultrahigh frequency resolution and tuning with programmable, stable, and accurate phase control. Figure 9 shows a schematic of the OCDMA coder/decoder. The coder/decoder circuit consists of a common input bus and a common output bus, with 4<sup>th</sup> order microring resonators serving as wavelength selective cross connects between the two. The ring radii were 47  $\mu\text{m}$ . A fourth order filter cell occupies an on-chip area of 100  $\mu\text{m}$  x 400  $\mu\text{m}$  allowing for a large number of filter cells to physically reside on a chip (64 filter cells on a 17mm x 17mm chip). Each filter is independently tunable in wavelength and each passband represents a frequency bin. In the

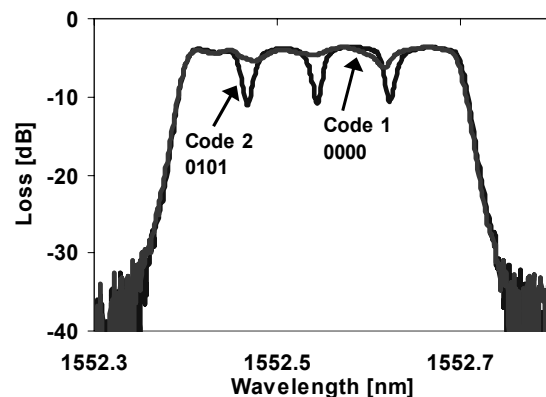


Figure 10. Composite spectral intensity response of the OCDMA circuit.

current generation, four bins are used. The bins are spaced by 10 GHz with each passband having a 3-dB bandwidth of 8 GHz. The passband widths of the filters can be adjusted by modifying the ring to ring coupling strengths. The relative phase shift between two adjacent frequency bins is controlled by a thermo-optic phase heater, shown hatched in Figure 9. The phase can be continuously varied between 0 and  $\pi$ . Figure 10 shows the composite response of the four narrowband channels. Multi-user system level transmission experiments we carried out, and showed the capability of sub  $10^{-9}$  bit error rates [6].

### High Bit Count Programmable True Time Delay Line

The high index platform allows the fabrication of very long waveguide in a small area while maintaining low loss. These long waveguides are ideal elements to provide different delays of the optical signal propagating in the PLC. Figure 11 shows the size of the fabricated long spiral waveguides with lengths between 0.5 and 1.5 meters. High bit count programmable true time delay line can be constructed using a combination of waveguides of various lengths and crossbar switches. The programmable delay line devices find application in microwave photonics for beam steering and shaping [7]. These devices can be fitted in less than a square centimeter and have delays controllable from 5 fsec to 10 nsec. Figure 12 shows an 8 bit programmable delay line device that consists of 9 crossbar switches and 8 delay elements. The measured delay values as a function of the bit setting for devices with delay resolutions  $\Delta T$  1, 4 and 8 ps are shown in Figure 13. The measured delay values are well within 1 % of the target. The



Figure 11 High index long waveguide spirals with lengths 0.5, 1.0 and 1.5 meters.

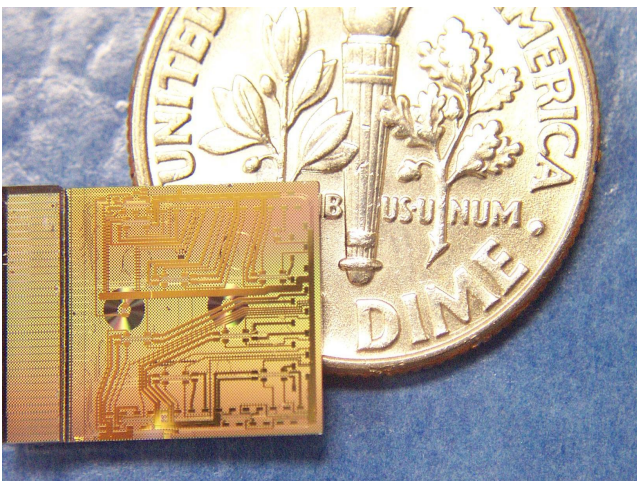


Figure 12 An 8-bit programmable delay line chip with 9 crossbar switches and 8 delay elements.

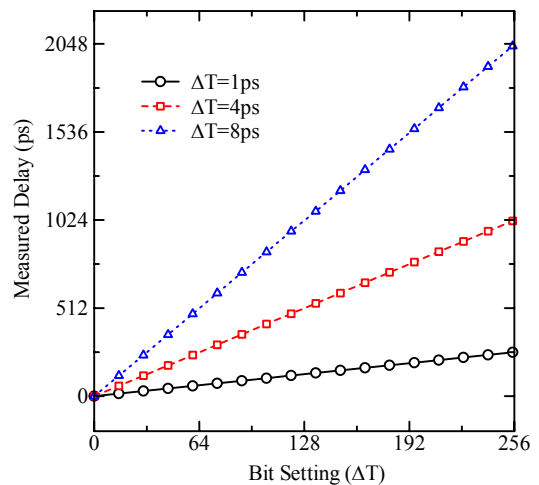


Figure 13 Measured group delay as a function of bit setting for three programmable delay line devices.

insertion losses of the devices are between 2.5 dB at 1 ps delay and 8.5dB at 2048 ps delay.

## Biosensing

An air-clad ring resonator has an evanescent field that can interact with the environment. Changes in the environment will cause changes in resonant wavelength or the field amplitude. Microring resonators present an ideal approach for optical transduction of environmental changes due to their small size and high Q. Photons in high Q rings make many round trips, and build up a strong signal to noise ratio. Due to their small size, tens of thousands of rings can be placed on a 1cm x 1cm chip. Micro-spotting technology exists in the field to functionalize this density of arrays.

Microrings are made selective to certain species by functionalizing the surface of the ring waveguide with receptors engineered to have a high affinity to their targets. Antibodies and proteins for example, have been widely used in sensors to detect certain pathogens.

A schematic of the surface of a functionalized ring resonator is shown in Figure 14a,

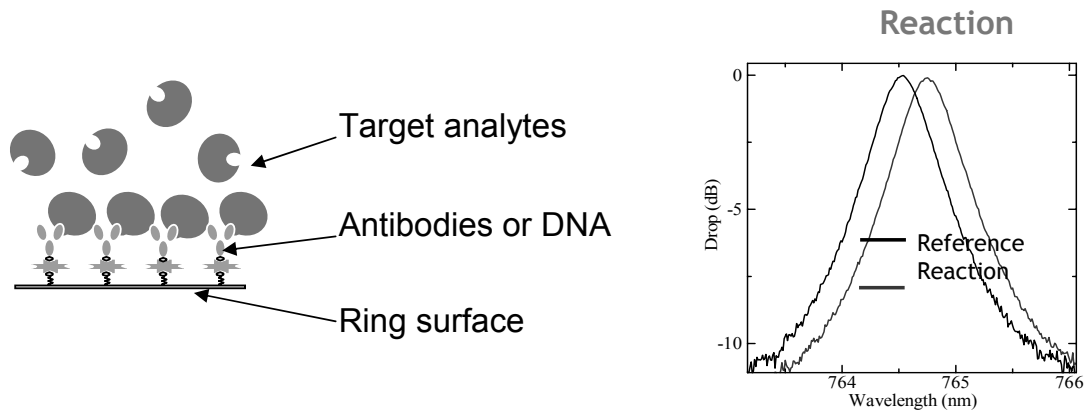


Figure 14. (a) Schematic close-up of the surface of a functionalized ring resonator. (b) Experimental results for the detection of surface binding between Biotin and Avidin.

while Figure 14b shows experimental data of a typical Biotin-Avidin reaction [8]. In this case Biotin was bound to the surface of the ring, while Avidin in a buffered solution flowed across the surface. The accumulation of Avidin binding to the Biotin at the surface of the ring causes a volumetric change in the environment, resulting in a detectable frequency shift.

## Conclusions

In summary, a robust high index contrast photonics platform for miniaturization, feature enhancement for optical signal processing has been introduced. In the next few years,

a new breed of highly integrated photonics circuit that find applications in a variety of areas can be expected.

### References

- [1] B. E. Little and S. T. Chu, *Toward Very Large-Scale Integrated Photonics*, Optics & Photonics News, pp 24-29, November 2000.
- [2] B. E. Little, "A VLSI Photonics Platform," *Proceedings of the Optical Fiber Communications Conference*, vol. 2, pp. 444-445, 2003.
- [3] S.J. Fiedziuszko and S. Holme, *Dielectric Resonators Raise your High-Q*, IEEE Microwave Magazine, pp. 50-60, September 2001.
- [4] S. T. Chu, B. E. Little, V. Van, J. V. Hryniewicz, P. P. Absil, F. G. Johnson, D. Gill, O. King, F. Seiferth, M. Trakalo, J. Shanton, "Compact full C-band tunable filters for 50 GHz channel spacing based on high order micro-ring resonators," *Optical Fiber Communication Conference*, 2004. OFC 2004, Volume: 2, 23-27 Feb. 2004.
- [5] S. Etemad et al., *IEEE Photon Techn Lett.*, to be published in April 2005.
- [6] A. Agarwal, P. Toliver, R. Menendez, S. Etemad, J. Jackel, J. Young, T. Banwell, B.E. Little, S. T. Chu, J. Hryniewicz, Wenlu Chen, Wei Chen, P. Delfyett "Fully-programmable ring resonator based integrated photonic circuit for phase coherent applications," *Proceedings of the Optical Fiber Communications Conference*, post-deadline paper, 2005.
- [7] Frigyes I, Seed, A.J, "Optically generated TTD in phase array antenna", *IEEE Trans. Microwave Theory & Technology*, v43, pp. 2378-2386, 1995.
- [8] J. Hryniewicz, N. Chbouki, B. E. Little, O. King, V. Van, S. Chu, and D. Gill, "Microring resonators: the promise of a powerful biochemical sensor platform," *Biophotonics/Optical Interconnects and VLSI Photonics/WBM Microcavities, 2004 Digest of the LEOS Summer Topical Meetings*, pp. 33-34, June 2004.